08

# Influence of metric parameters on the electrical conductivity properties of thin films of perforated graphene functionalized with carboxyl groups

© P.V. Barkov,[1] M.M. Slepchenkov,[1] O.E. Glukhova[1,2]

[1]Saratov National Research State University,
410012 Saratov, Russia
[2]I.M. Sechenov First Moscow State Medical University,
119992 Moscow, Russia
e-mail: barkovssu@mail.ru

*Received December 26, 2024*
*Revised December 26, 2024*
*Accepted December 26, 2024*

Using the density functional theory based tight binding method, we have *in silico* studied of the electrical conductivity properties of thin films of perforated graphene with almost circular holes with a diameter of 1.2 nm and a neck width of 0.7−2 nm. Patterns in the change of the electrical conductivity of the investigated films with increasing neck width in different directions of the hexagonal graphene lattice were identified. It was found that when the neck width was altered in „zigzag" direction, the electrical conductivity changed abruptly in steps of three, while in „armchair" direction it increased nearly linearly. To explain the observed patterns, the characteristics of quantum electron transport in the studied films at various neck widths were analyzed.

**Keywords:** electrical conductivity, density functional theory based tight binding method, neck width, electron transmission function.

DOI: 10.61011/TP.2025.05.61127.464-24

## Introduction

One of the new fields of materials science is the study of perforated two-dimensional ($2D$) nanomaterials [1]. Among $2D$-perforated nanomaterials, one of the most promising and demanded is perforated graphene (PG), which is a graphene structure with a periodic array of holes of different sizes and shapes with different spacing [2]. The structural features of PG are characterized by two key geometric parameters:

1) „periodicity", defined as a distance between the centers of two adjacent holes;

2) „cell width" (W) defined as the lowest value between the edges of two neighboring holes [3,4].

Modern synthesis technologies such as nanolithography, catalytic oxidation/hydrogenation, photocatalytic cutting, electrochemical pattern formation, and direct electron/ion beam irradiation make it possible to obtain GP structures with geometric parameters that vary widely [5]. Researchers' close attention to PG is explained by its high specific surface area with a large number of useful reaction/adsorption centers, significantly improved mass and charge transfer, electronic structure with a tunable band gap, as well as excellent mechanical, magnetic, and photocatalytic properties [6,7]. Due to a variety of the properties listed above, PG may be used in many different technical fields [8,9]. In particular, PG is considered as a promising candidate for replacement of graphene nanoribbons in creation of field-effect transistors [10]. In paper [3] using block copolymer lithography, the PG-based field-effect transistors were manufactured, for which it was experimentally established that the ratio of on and off currents $I_{on}/I_{off}$ of the device can be adjusted by changing the width of PG neck. In particular, with the width of neck 7 nm the coefficient $I_{on}/I_{off}$ was more than 100. Field-effect transistors based on PG nanoribbons with a width of less than 10 nm, synthesized using nanoimprint lithography, are proposed in this paper [11]. It has been shown that by reducing the width of PG nanoribbons, it is possible to achieve an increase in $I_{on}/I_{off}$ coefficient of transistor. Compared to pure graphene, PG structures are characterized by faster transverse ion diffusion, which makes them a promising electrode material for energy storage devices with improved performance. For example, the specific capacity of pure PG in a non-aqueous electrolyte is 1.4 times higher than that of pure graphene [12], and in aqueous electrolytes — it is 1.5 times higher than that of pure graphene [13]. It is possible to increase the specific capacity of PG-based electrode, and hence improve energy storage efficiency, by alloying the PG with other elements, including nitrogen, phosphorus, and sulfur [14–16].

For the effective use of PG in electronic devices such as transistors and sensors, it is important to be able to fine-tune the electronic and electrically conductive properties of PG-based nanomaterials. One of the possible ways to solve this problem is to select the optimal geometric parameters of PG, providing the required electronic and electrically conductive properties. Using methods *ab initio* the size of PG energy slit was predicted to be capable of being tuned by varying the width of the neck, shape and diameter of hole, as well as location of holes along „zigzag" direction or „armchair" direction of graphene hexagonal

lattice [17]. In [18], using the method of density functional theory (DFT), it was shown that PG films with almost round holes are characterized by the largest energy gap compared to PG films with triangular and rectangular holes. Another way to manage PG properties is through functionalization.

Currently, studies are being conducted to identify the patterns of influence of various gas molecules on the electron-energy and sensory characteristics of PG [19–21]. At the same time, these studies consider the situation when gas molecules are adsorbed on a clean surface of a PG. However, experiments on the synthesis of PG, as well as an ordinary decanter, have shown the obligatory presence of oxygen-containing groups [22,23]. These groups should influence the electronic structure and electron-energy parameters of PG due to high electronegativity of oxygen. Earlier we studied the influence of C=O-groups on electronegativity of PG films with various neck width [24]. The purpose of this work is to identify patterns of the influence of neck width on the electrically conductive characteristics of PG films functionalized with carboxylic COOH-groups. The object of the study is thin films of PG with holes of almost circular shape with a diameter of 1.2 nm.

## 1. Research methods

The study was conducted using the density functional theory formalism in the self-consistent charge density-functional tight-binding approximation (SCC DFTB) [25] using open-source software DFTB+ [26,27]. The SCC DFTB method is chosen due to the polyatomic nature of the calculated supercells, which contain several hundred atoms. The equilibrium configuration of thin film supercells within the framework of optimization was searched until the values of interatomic forces became less than $10^{-4}$ eV·Å$^{-1}$. The reciprocal space was partitioned according to the Monkhorst–Pack scheme [28] using a mesh of $k$-points with a size of $4 \times 4 \times 1$ for optimization of the atomic structure of supercells.

The electrical conductivity of the studied structures was calculated within the framework of the Landauer–Butticker formalism [29] according to the following formula

$$G = 2e^2/h \int_{-\infty}^{\infty} T(E)F_T(E - E_F)dE, \quad (1)$$

where $T(E)$ — average electron transmission function, $E_F$ — Fermi level of the electrodes, $e^2/h$ — quantum of conductivity, $F_T$ — function of thermal broadening of energy levels, defined as

$$F_T = \frac{1}{4k_BT} sech^2\left(\frac{E - E_F}{2k_BT}\right). \quad (2)$$

The coefficient 2 before the integral in formula (1) takes into account the spin. The electron transmission function $T(E, k)$ is expressed as follows

$$T(E, k) = Tr\left(\Gamma_S(E, k)G_C^A(E, k)\Gamma_D(E, k)G_C^R(E, k)\right), \quad (3)$$

where $G_C^A(E, k)$ and $G_C^R(E, k)$ — leading and lagging Green's matrices describing the interaction of the simulated system with electrodes, and $\Gamma_S(E, k)$ and $\Gamma_D(E, k)$ — expansion matrices of electronic states of the source and drain electrodes. The electric conductivity of the studied films were calculated in the basis $s$- and $p$-of electronic orbitals at a temperature of 300 K.

## 2. Construction of supercells of the films of functionalized PG

The initial supercell of PG film consisting of 186 carbon atoms was $2.46 \times 2.55$ nm in size (in $X$ and $Y$ axes) and the hole diameter $\sim 1.2$ nm (Fig. 1, $a$). The neck width was 0.74 nm in „zigzag“ direction ($X$ axis) and 0.99 nm in „armchair“ direction ($Y$ axis) of graphene lattice. The selected metric parameters correspond to the known experimental data on PG synthesis [30,31]. PG supercells with the increasing neck width in direction of $X$ and $Y$ axes ($W_X$ and $W_Y$) was built on the basis of initial supercell as follows:

1) the neck width $W_X$ changed from 0.74 to 2.22 nm with a spacing $\Delta W_X = 0.24$ nm, at that the neck width $W_Y$ was equal 0.99 nm;

2) the neck width $W_Y$ changed from 0.99 to 2.27 nm with a spacing $\Delta W_Y = 0.42$ nm, at that the neck width $W_X$ remained equal 0.74 nm (Fig. 1, $b$). In total, we used 10 different supercells of PG to conduct our research.

The functional COOH-groups were covalently attached to PG atoms located at the edges of the hole, since unsaturated carbon bonds are present in this region. The modeling of the functionalization process was carried out step by step using the original methodology described in detail in this paper [32]. According to this method, the atom with the largest excess negative charge was selected for the addition of COOH-group based on the partial

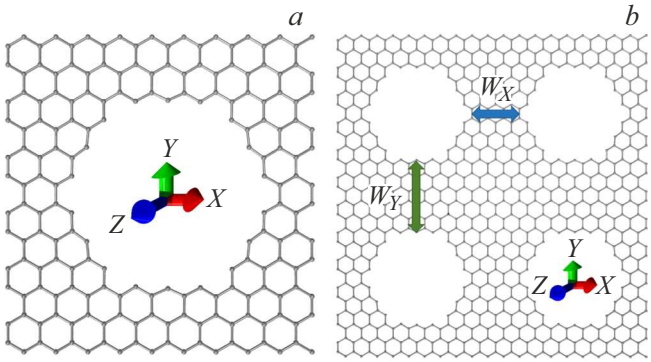


**Figure 1.** Initial PG supercell with a size of $2.46 \times 2.55$ nm ($a$) and extended fragment of this supercell with designation of the neck width along „zigzag“ ($W_X = 0.74$ nm) and along „armchair“ ($W_Y = 0.99$ nm) ($b$).

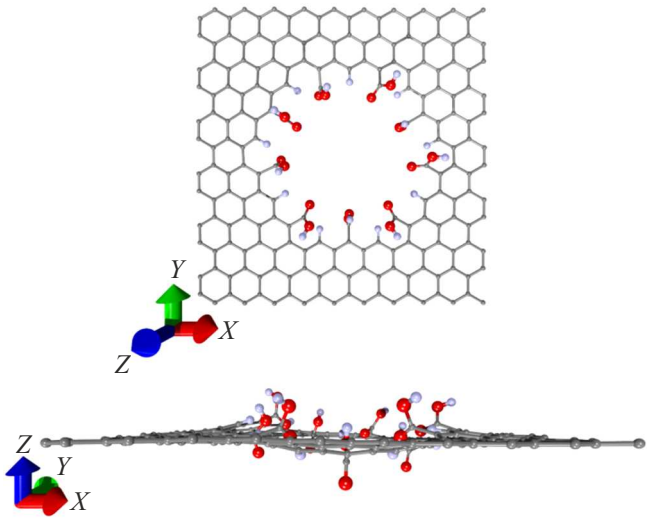


**Figure 2.** Equilibrium atomic configuration of initial PG supercell (size $2.46 \times 2.55$ nm, neck width $W_X = 0.74$ nm, $W_Y = 0.99$ nm) with nine attached COOH-groups (plan view and side view).

charge distribution calculated using Mulliken method for all atoms of the supercell, and after adding each new functional group, this distribution was recalculated. Figure 2 shows the equilibrium atomic configuration of the initial PG supercell with nine COOH-groups attached (top view and side view). As can be seen from the figure, the nearest neighbors of PG atoms to which COOH-groups were attached are saturated with hydrogen atoms. This was done in order to avoid formation of unnecessary covalent bonds between functional groups and the nearest neighboring carbon atoms. Similarly, COOH- was functionalized by groups of other PG super cells with increasing values of $W_X$ and $W_Y$.

During numerical experiments on the covalent attachment of COOH-groups to PG atoms, the binding energy $E_b$ was estimated according to the formula

$$E_b = E_{PG+n\mathrm{COOH}+mH} - E_G - E_{n\mathrm{COOH}} - E_{mH}, \qquad (4)$$

where $E_{PG+n\mathrm{COOH}} + mH$ — energy of PG supercell with attached COOH-groups ($n$ — number of groups) and attached hydrogen atoms ($m$ — number of fixed hydrogen atoms), $E_{PG}$, $E_{n\mathrm{COOH}}$, $E_{mH}$ — energies of isolated PG, COOH-groups and hydrogen atoms, respectively. The calculation results showed that at different stages of functionalization, $E_b$ takes values in the range from $-80$ to $-20$ MeV/atom. Negative values of $E_b$ indicate that the process of covalent attachment of COOH-groups to atoms at the edges of PG hole is energetically advantageous, and the resulting atomic configurations of the functionalized PG are distinguished by thermodynamic stability.

## 3. Electrically conductive properties of functionalized PG films with variable neck width

Electric conductivity of PG films within this study was assessed by the value of conductivity $\sigma$ calculated for the two directions of the current transport: along „zigzag“ ($X$) and along „armchair“ directions ($Y$ axis) of graphene hexagonal lattice. Before proceeding to the discussion of the dependencies of $\sigma$ on the neck width for PG with COOH-groups, let us recall the already well-known pattern of changes in $\sigma$ with the growth of $W_X$ and $W_Y$ for non-functionalized PG, found in our previous study [33]:

1) PG structures are characterized by anisotropy of electrical conductivity caused by non-uniform distribution of the local density of electronic states (LDOS) across

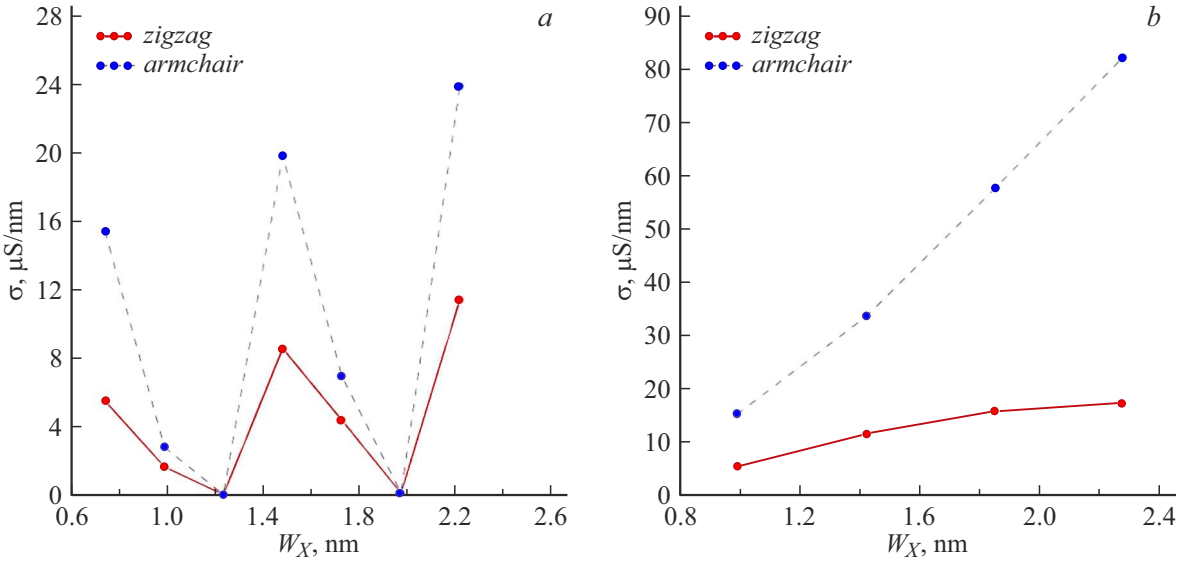


**Figure 3.** Curves of conductivity of $\sigma$ PG, functionalized by COOH-groups versus neck width when it is increasing along „zigzag“ ($a$) and „armchair“ ($b$) directions for different directions of the current transport („zigzag“ and „armchair“).

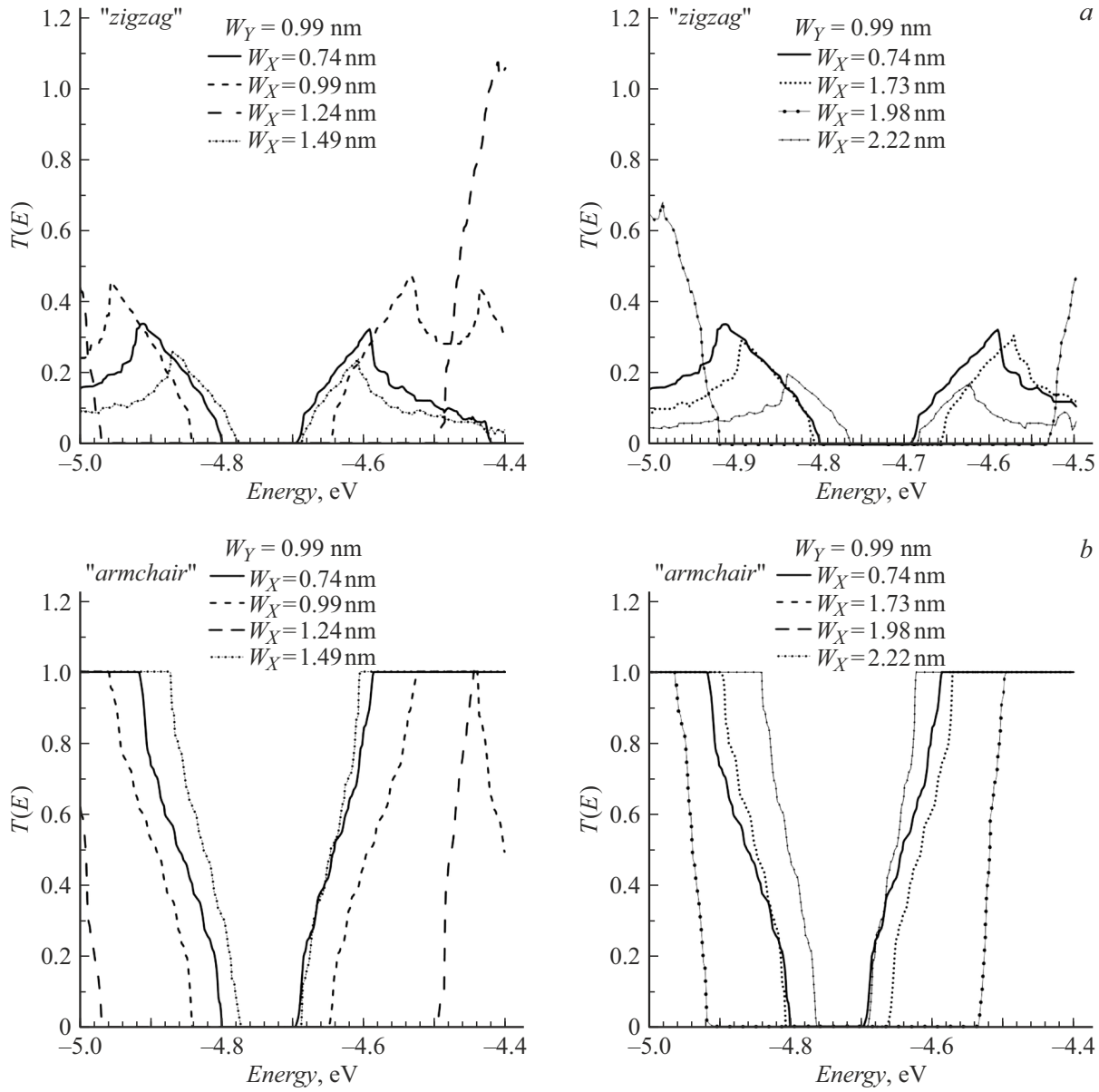


**Figure 4.** Functions of transmission of PG functionalized with COOH-groups, in „zigzag“ ($a$) and „armchair“ directions of the current transport ($b$) at fixed value of the neck width $W_Y = 0.99$ nm and values of the neck width $W_X$, varying in the range from 0.74 to 2.22 nm.

the atoms of PG supercell along „armchair“ and „zigzag“ directions;

2) with an increase of $W_X$, the value $\sigma$ demonstrates the abrupt nature of change in both directions of current transport, while with an increase in $W_Y$ $\sigma$ it changes almost monotonously.

Let's now find out how $\sigma$ will change with an increase in the neck width for PG in the presence of COOH-groups. Fig. 3 illustrates the dependences $\sigma(W_X)$ (Fig. 3, $a$) and $\sigma(W_Y)$ (Fig. 3, $b$) for the supercells of the functionalized PG. It can also be noted that the nature of change $\sigma$ of the functionalized PG, in general, is similar to the dependences $\sigma(W_X)$ and $\sigma(W_Y)$ described in [33] for PG with no COOH-groups. With an increase in the width of the neck $W_X$, the value of $\sigma$ changes abruptly (Fig. 3, $a$) in both directions of current transport. The jumps step is equal to three, whereas at $W_X = 1.24$ nm and $W_X = 1.98$ nm $\sigma$ it is decreased almost to zero (below 0.1 $\mu$S/nm). With an increase in the neck width $W_Y$, the value of $\sigma$ does not change by jumps, but demonstrates growth close to linear (Fig. 3, $b$). Also the conductivity anisotropy persists: the difference in values $\sigma$ between „armchair“ and „zigzag“ directions of the current transport makes $\sim 3$ times for the initial supercell with minimal sizes $W_X$ and $W_Y$, and with enlarged neck width $W_X$ this difference declines by 2 times in the maxima, with the neck width growth $W_Y$ it rises up to 5 times. Compared to non-functionalized PG, only the values assumed by the electrical conductivity

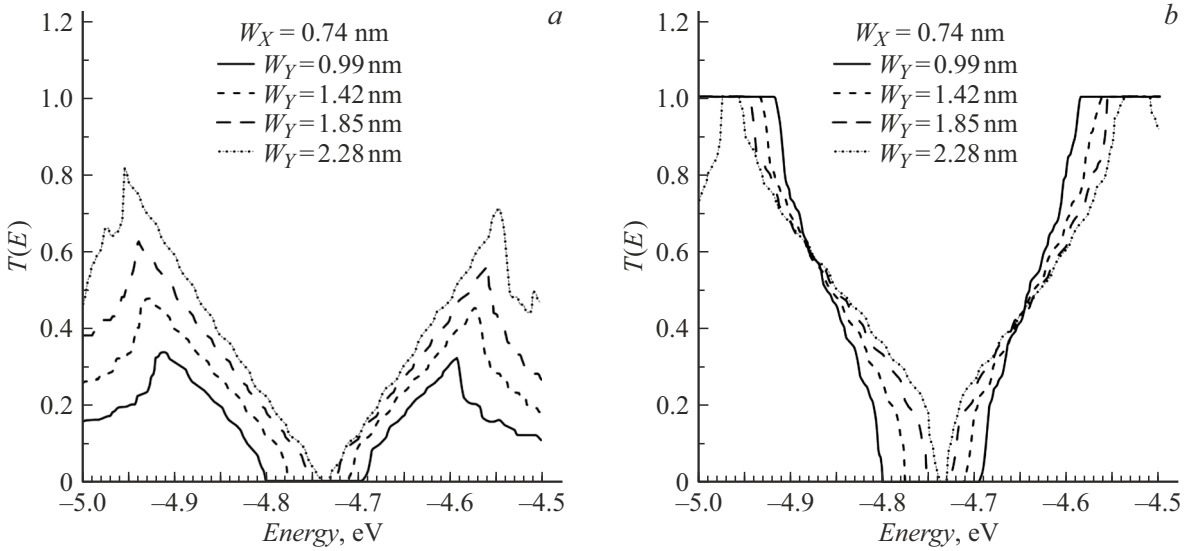


**Figure 5.** Functions of transmission of PG functionalized with COOH-groups, in „zigzag“ ($a$) and „armchair“ directions of the current transport ($b$) at fixed value of the neck width $W_X = 0.74$ nm and values of the neck width $W_Y$, varying in the range from 0.99 to 2.28 nm.

$\sigma$ are changing. In particular, with the enlarged neck width $W_X$ the maxima $\sigma$ take values $15-24\,\mu$S/nm for the functionalized PG and $46-54\,\mu$S/nm for the non-functionalized PG with current transport along „armchair“ direction, whereas with current transport along „zigzag“ the values $\sigma$ make $5-11\,\mu$S/nm for the functionalized PG and $15-21\,\mu$S/nm for the non-functionalized PG. The difference in values $\sigma$ between non-functionalized and functionalized PG is explained by the phenomenon of charge transfer from PG atoms to COOH-groups described in [32] during formation of a covalent compound between them. In turn, the electrical conductivity $\sigma$ of both functionalized and non-functionalized PG is higher than that of a conventional graphene sheet ($\sim 3\,\mu$S/nm in both directions of current transport according to our SCCDFTB-calculations).

To explain the patterns of behavior observed in Fig. 3 $\sigma$, including quantitative changes in the ratios of values $\sigma$ between the two directions of current transport, we present graphs of the electron transmission function $T(E)$ for supercells of functionalized PG with different neck widths $W_X$ and $W_Y$. Fig. 4 shows the dependencies $T(E)$ for the case of enlarged neck width $W_X$. It can be clearly seen that the stepwise change of $\sigma$ in Fig. 3, $a$ is explained by the expansion or narrowing of the transport slit (the length of the energy range in which $T(E)$ becomes zero) at different values of the neck width $W_X$ (Fig. 4, $a$). In particular, at $W_X = 1.24$ and 1.98 nm, when $\sigma$ drops to almost zero, the width of the transport slit in both directions of current transport is 0.48 and 0.38 eV, respectively, while at the maximum points $\sigma$ it is on the order of 0.1 eV and less. It also follows from Fig. 4 that the values $T(E)$ near the Fermi level (4.72–4.74 eV depending on the values of $W_X$ and $W_Y$) in„armchair“ direction of the current transport is several times larger than in „zigzag“ direction. For example, at $W_X = 0.74$ nm and $W_Y = 0.99$ nm (initial PG supercell) the values $T(E)$ in „armchair“ and „zigzag“ directions differ by $\sim 3$ times, and at $W_X = 1.98$ nm and $W_Y = 0.99$ nm — it differs already by $\sim 2$ times, which explains the anisotropy of conductivity in Fig. 3.

Fig. 5 shows the dependencies $T(E)$ for the case of enlarged neck width $W_Y$. It can be seen from the graphs in Fig.5 that both in case of current transport along „zigzag“ direction and current transport along „armchair“ direction, a narrowing of the width of the transport slit is observed, and the magnitude of this narrowing is proportional to the increase in the coefficient showing the ratio between the values $\sigma$ in two directions of the current transport. Thus, at $W_X = 0.74$ nm and $W_Y = 1.42$ nm the transport slit makes $\sim 0.06$ eV, which corresponds to the almost threefold increase of $\sigma$ in „armchair“ direction compared to „zigzag“ direction, and at $W_X = 0.74$ nm and $W_Y = 2.28$ nm the transport slit $\sim 0.01$ eV corresponds to the difference by $\sim 4.8$ times between the values $\sigma$ in different directions of the current transport. In addition, as in the case of widened neck width $W_X$, it can be noted that the number of available conductivity channels, determined by the value of function $T(E)$, differs between „zigzag“ and „armchair“ directions of current transport in favor of the latter.

Thus, based on the analysis, it can be concluded that the electrically conductive properties of PG films functionalized with COOH-groups can be enhanced or weakened by varying the width of the neck.

## Conclusion

Thus, based on the results of SCC DFTB calculations, patterns of the neck width effect on the conductivity of thin films of PG functionalized with COOH-groups along

the edges of almost round holes with a diameter of 1.2nm were revealed. The analysis of conductivity graphs $\sigma$ of the studied films with different metric parameters showed that by varying the neck width in „zigzag“ direction, the effect of switching current between states with high and almost zero conductivity can be realized in the structures of the functionalized PG, and by changing the neck width in „armour“ direction, it is possible to achieve multiple (4–5) increase of $\sigma$, which is critical for the operation of transistor and sensor devices based on similar graphene nanomaterials.

### Funding

This work was supported by a grant from the Russian Science Foundation (project No. 23-72-01122, https://rscf.ru/project/23-72-01122/).

### Conflict of interest

The authors declare that they have no conflict of interest.

## References

[1] D. Wang, Y. Dou, X. Zhang, K. Bi, I.R. Panneerselvam, H. Sun, X. Jiang, R. Dai, K. Song, H. Zhuang, Y. Lu, Y. Wang, Y. Liao, L. Ding, Q. Nian. Nano Today, **55**, 102162 (2024). DOI: 10.1016/j.nantod.2024.102162
[2] M. Nazarian-Samani, S. Haghighat-Shishavan, M. Nazarian-Samani, S.F. Kashani-Bozorg, S. Ramakrishna, K.B. Kim. Progr. Mater. Sci., **116**, 100716 (2021). DOI: 10.1016/j.pmatsci.2020.100716
[3] J. Bai, X. Zhong, S. Jiang, Y. Huang, X. Duan. Nat Nanotechnol., **5**, 190 (2010). DOI: 10.1038/nnano.2010.8
[4] J. Yanga, M. Maa, L. Lia, Y. Zhanga, W. Huanga, X. Dong. Nanoscale, **6**, 13301 (2014). DOI: 10.1039/C4NR04584J
[5] N.S. Rajput, S.A. Zadjali, M. Gutierrez, A.M.K. Esawi, M.A. Teneiji. RSC Adv., **11**, 27381 (2021). DOI: 10.1039/d1ra05157a
[6] R. Ma, Y. Zhou, H. Bi, M. Yang, J. Wang, Q. Liu, F. Huang. Progr. Mater. Sci., **113**, 100665 (2020). DOI: 10.1016/j.pmatsci.2020.100665
[7] Y. Lin, Y. Liao, Z. Chen, J.W. Connell, Mater. Res. Lett., **5** (4), 209 (2017). DOI: 10.1080/21663831.2016.1271047
[8] T. Liu, L. Zhang, B. Cheng, X. Hu, J. Yu. Cell Reports Phys. Sci., **1**, 100215 (2020). DOI: 10.1016/j.xcrp.2020.100215
[9] K. Yanga, J. Lia, L. Zhou, T. Zhang, L. Fu. Flat Chem., **15**, 100109 (2019). DOI: 10.1016/j.flatc.2019.100109
[10] M. Kim, N.S. Safron, E. Han, M.S. Arnold, P. Gopalan. Nano Lett., **10**, 1125 (2010). DOI: 10.1021/nl9032318
[11] X. Liang, Y.S. Jung, S. Wu, A. Ismach, D.L. Olynick, S. Cabrini, J. Bokor. Nano Lett., **10**, 2454 (2010). DOI: 10.1021/nl100750v
[12] C.-H. Yang, P.-L. Huang, X.-F. Luo, C.-H. Wang, C. Li, Y.-H. Wu, J.-K. Chang. Chem. Sus. Chem., **8**, 1779 (2015). DOI: 10.1002/cssc.201500030
[13] K.A. Sammed, L. Pan, M. Asif, M. Usman, T. Cong, F. Amjad, M.A. Imran. Sci. Rep., **10**, 2315 (2020). DOI: 10.1038/s41598-020-58162-9
[14] F. Su, S. Zheng, F. Liu, X. Zhang, F. Su, Z.-S. Wu. Chin. Chem. Lett., **32**, 914 (2021). DOI: 10.1016/j.cclet.2020.07.025
[15] J.H. Jeong, G.-W. Lee, Y.H. Kim, Y.J. Choi, K.C. Roh, K.-B. Kim. Chem. Eng. J., **378**, 122126 (2019). DOI: 10.1016/j.cej.2019.122126
[16] D. Yang, B. Xu, Q. Zhao, X.S. Zhao. J. Mater. Chem. A, **7**, 363 (2019). DOI: 10.1039/C8TA09188A
[17] W. Oswald, Z. Wu. Phys. Rev. B, **85**, 115431 (2012). DOI: 10.1103/PhysRevB.85.115431
[18] G. Tang, Z. Zhang, X. Deng, Z. Fan, Y. Zeng, J. Zhou. Carbon, **76**, 348 (2014). DOI: 10.1016/j.carbon.2014.04.086
[19] M.S. Eldeeb, M.M. Fadlallah, G.J. Martyna, A.A. Maarouf. Carbon, **133**, 369 (2018). DOI: 10.1016/j.carbon.2018.03.048
[20] L. Huang, S. Miao, X. Wang, X. Yang. Molecular Simulation, **46**, 853 (2020). DOI: 10.1080/08927022.2020.1778171
[21] M.K. Rabchinskii, S.D. Saveliev, D.Yu. Stolyarova, M. Brzhezinskaya, D.A. Kirilenko, M.V. Baidakova, S.A. Ryzhkov, V.V. Shnitov, V.V. Sysoev, P.N. Brunkov. Carbon, **182**, 593 (2021). DOI: 10.1016/j.carbon.2021.06.057
[22] V.V. Shnitov, M.K. Rabchinskii, M. Brzhezinskaya, D.Yu. Stolyarova, S.V. Pavlov, M.V. Baidakova, A.V. Shvidchenko, V.A. Kislenko, S.A. Kislenko, P.N. Brunkov. Small, **17**, 2104316 (2021). DOI: 10.1002/smll.202104316
[23] P.V. Barkov, M.M. Slepchenkov, O.E. Glukhova. Technical Physics, **69** (4), 404 (2024).
[24] M. Elstner, D. Porezag, G. Jungnickel, J. Elsner, M. Haugk, Th. Frauenheim, S. Suhai, G. Seifert. Phys. Rev. B, **58**, 7260 (1998). DOI: 10.1103/PhysRevB.58.7260
[25] B. Aradi, B. Hourahine, Th. Frauenheim. J. Phys. Chem. A, **111**, 5678 (2007). DOI: 10.1021/jp070186p
[26] B. Hourahine, B. Aradi, V. Blum, F. Bonafé, A. Buccheri, C. Camacho, C. Cevallos, M.Y. Deshaye, T. Dumitrică, A. Dominguez, S. Ehlert, M. Elstner, T. van der Heide, J. Hermann, S. Irle, J.J. Kranz, C. Köhler, T. Kowalczyk, T. Kubař, I.S. Lee, V. Lutsker, R.J. Maurer, S.K. Min, I. Mitchell, C. Negre, T.A. Niehaus, A.M.N. Niklasson, A.J. Page, A. Pecchia, G. Penazzi, M.P. Persson, J. Řezáč, C.G. Sánchez, M. Sternberg, M. Stöhr, F. Stuckenberg, A. Tkatchenko, V. W.-Z. Yu, T. Frauenheim. J. Chem. Phys., **152**, 20 (2020). DOI: 10.1063/1.5143190
[27] M. Elstner, G. Seifert. Philos. Trans. R. Soc. A, **372**, 20120483 (2014). DOI: 10.1098/rsta.2012.0483
[28] H.J. Monkhorst, J.D. Pack. Phys. Rev. B, **13**, 5188 (1976). DOI: 10.1103/PhysRevB.13.5188
[29] S. Datta. *Quantum Transport: Atom to Transistor* (Cambridge University Press, London, UK, 2005), p. 404.
[30] M.K. Rabchinskii, V.V. Shnitov, A.T. Dideikin, A.E. Aleksenskii, S.P. Vul, M.V. Baidakova, I.I. Pronin, D.A. Kirilenko, P.N. Brunkov, J. Weise, S.L. Molodtsov. J. Phys. Chem. C, **12**, 28261 (2016). DOI: 10.1021/acs.jpcc.6b08758
[31] B. Sakkaki, H.R. Saghai, G. Darvish, M. Khatir. Opt. Mater., **122**, 111707 (2021). DOI: 10.1016/j.optmat.2021.111707
[32] O.E. Glukhova, P.V. Barkov. Lett. Mater., **12**, 392 (2021). DOI: 10.22226/2410-3535-2021-4-392-396
[33] P.V. Barkov, O.E. Glukhova. Nanomaterials, **11**, 1074 (2021). DOI: 10.3390/nano11051074

*Translated by T.Zorina*